

Luminescent Organic 1D Nanomaterials Based on Bis(β -diketone)carbazole Derivatives

Xingliang Liu,^[a] Defang Xu,^[a] Ran Lu,^{*[a]} Bin Li,^[b] Chong Qian,^[a] Pengchong Xue,^[a] Xiaofei Zhang,^[a] and Huipeng Zhou^[a]

Abstract: A series of new triphenylamine-functionalized bis(β -diketone)s bridged by a carbazole (C_n BDKC, $n = 1, 4, 8, 16$) with twisted intramolecular charge-transfer emission in polar solvents has been synthesized. The length of the carbon chains has a significant effect on the self-assembling properties of the compounds. Well-defined 1D nanowires were easily generated from C1BDKC with a methyl group by a reprecipitation approach directed by π -stacking interaction, and the molecules packed into J-aggregates in the nano-

wires. In addition, 1D nanofibers based on C16BDKC bearing a long hexadecyl chain were prepared through the organogelation process, and H-aggregates were formed driven by the synergistic effect of π -stacking interaction and van der Waals force in the gel phase. C4BDKC and C8BDKC containing butyl and octyl side chains, respective-

ly, cannot arrange into dispersed nanostructures, probably because π - π interaction between conjugated moieties might be disturbed by the interaction between the side chains, which is, however, not strong enough to dominate the self-assembling process. Notably, the nanowires based on C1BDKC and the gel nanofibers from C16BDKC can emit strong green light under irradiation, which suggests that these 1D nanomaterials may have potential applications in emitting materials as well as photonic devices.

Keywords: ketones • luminescence • nanostructures • self-assembly • supramolecular chemistry


Introduction

During the past few years, nanostructures based on π -conjugated organic molecules have become the subject of ever-in-

creasing attention, as a result of the unique optical and optoelectronic properties superior to those of their bulk counterparts.^[1–3] Compared with zero-dimensional (0D) organic nanoparticles,^[4,5] one-dimensional (1D) nanomaterials^[6,7] are more promising building blocks for nanoscale devices, such as organic field-effect transistors (OFETs),^[8] solar cells,^[9] and nanoscale optical waveguides.^[6b,10] Recently, Zang et al. have fabricated 1D nanowires from perylene-based n-type semiconductor molecules that possess highly polarized, self-waveguided emission, which makes them ideal candidates for application in nanolasers and other angle-dependent optical nanodevices.^[10e,11] Yao's group has generated nanoribbon assemblies with multicolor emission from 1,2,3,4,5-pentaphenyl-1,3-cyclopentadiene dye.^[12] Ajayaghosh and co-workers have prepared white-light-limiting nanofibers through controlling the donor self-assembly and modulation of excitation energy transfer.^[13] Although great efforts have been made to construct 1D organic nanomaterials, the understanding of the factors affecting self-assembly, the final morphology of the fabricated nanomaterials, and the dependence of molecular arrangement on the optoelectronic properties (e.g., emission, exciton migration, and charge transport) of the assembled materials is still challenging. Therefore, the design of new organic building

[a] X. Liu, D. Xu, Prof. R. Lu, C. Qian, Dr. P. Xue, X. Zhang, H. Zhou
Key Laboratory of Supramolecular Structure
and Materials College of Chemistry
Jilin University
Changchun (P. R. China)
Fax: (+86) 431-88923907
E-mail: luran@mail.jlu.edu.cn

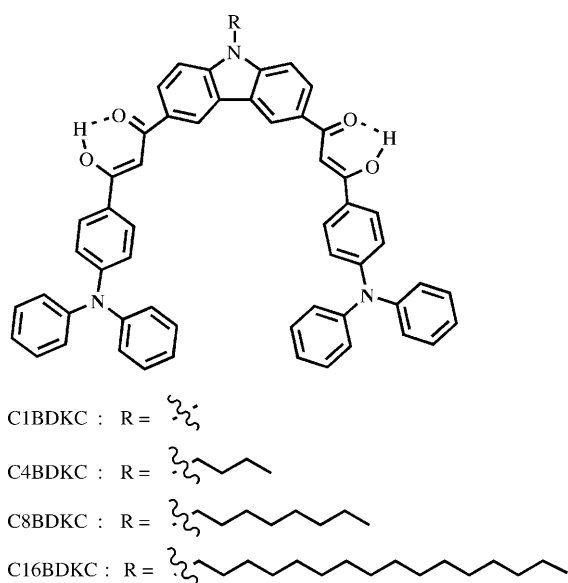
[b] Prof. B. Li
Key Laboratory of Excited State Processes
Changchun Institute of Optics, Fine Mechanics and Physics
Chinese Academy of Sciences
Changchun 130033 (P. R. China)

 Supporting information (¹H and ¹³C NMR spectra and MALDI-TOF mass spectra for all new compounds; UV/Vis absorption and fluorescence spectra; fluorescence decay profiles; SEM, TEM, fluorescence microscopy, and AFM images of the obtained nanomaterials; photographs of C16BDKC in different solvents under UV light; FTIR spectra of the xerogel; and ground-state geometry of C16BDKC by semiempirical calculations) for this article is available on the WWW under <http://dx.doi.org/10.1002/chem.201001858>.

blocks and the development of self-assembly approaches for the fabrication of 1D nanostructures with desired functionality should be focused on.

In addition, β -diketones have attracted current attention in organic, inorganic, and materials chemistry on account of their conventional chelation with cations, including metal or boron ions, to yield complexes with high fluorescence emission,^[14–16] and their high condensation reaction reactivity to provide convenient synthetic pathways to different classes of molecules.^[17,18] In particular, the formation of the hydrogen-bonded six-membered ring through O–H stretching modes from tautomerization between the ketone and enol forms would increase the molecular planarity, thus leading to the inhibition of the nonradiative dissipation. Therefore, if π -conjugated moieties are connected to β -diketones, the rigid hydrogen-bonded six-membered ring would be helpful for the molecular self-assembly directed by π -stacking interaction along the 1D direction. To date, self-assembled nanostructures based on β -diketone derivatives have not been extensively studied, although Yao and co-workers have fabricated dibenzoylmethane-based nanotubes of different sizes by using the immersion technique with a porous alumina membrane as the template.^[19] Therefore, the construction of 1D self-assemblies of β -diketone derivatives by a more straightforward method remains challenging.

Herein, we report the facile fabrication of 1D organic nanostructures with controllable morphology through the self-assembly of new triphenylamine-functionalized bis(β -diketone)s bridged by carbazole (C_n BDKC, $n=1, 4, 8, 16$) with alkyl chains of different length (Scheme 1) by a reprecipitation approach and organogelation, which are suggested as simple and mild ways to generate 1D organic nanomaterials. It is found that the length of the side chains has an effect on the self-assemblies of C_n BDKC. For instance,



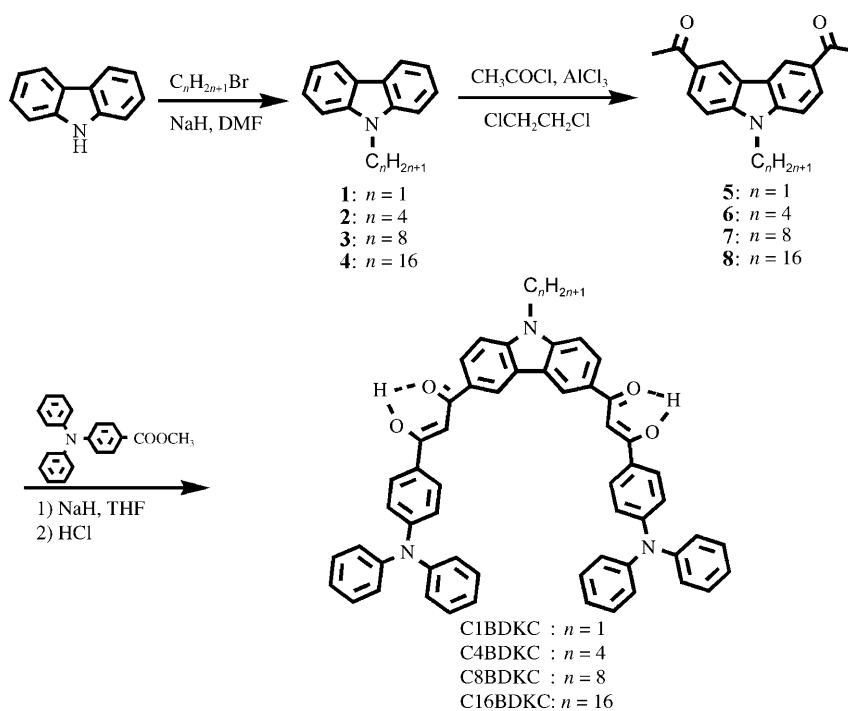
Scheme 1. Molecular structures of C1BDKC, C4BDKC, C8BDKC, and C16BDKC.

well-defined 1D nanowires with high monodispersities in both shape and size have been obtained from C1BDKC with a methyl group, whereas 1D nanofibers, which are thinner than C1BDKC-based nanowires, were generated from C16BDKC with a hexadecyl group through organogelation. The other compounds, C4BDKC and C8BDKC containing butyl and octyl groups, respectively, produced ill-defined agglomerates rather than 1D nanostructures. It should be noted that the 1D nanostructures based on C1BDKC and C16BDKC can give strong green fluorescent emission, which may indicate potential applications in emitting materials, fluorescent chemosensors, and so on.

Results and Discussion

Synthesis and characterization: The synthetic routes for triphenylamine-functionalized bis(β -diketone)s bridged by carbazole C_n BDKC ($n=1, 4, 8, 16$) are shown in Scheme 2. Firstly, the 3,6-diacetyl carbazoles **5–8** with different length carbon chains were synthesized by Friedel–Crafts reactions of *N*-alkyl-substituted carbazoles **1–4**, respectively,^[15e,20] which were obtained by the alkylation of carbazole with alkyl halide catalyzed by NaH in DMF in yields of over 90%.^[21] The target molecules of C1BDKC, C4BDKC, C8BDKC, and C16BDKC were prepared by Claisen condensation between methyl 4-(diphenylamino)benzoate and the corresponding diacetyl-substituted carbazoles **5–8** in the presence of sodium hydride in anhydrous THF, followed by acidification with dilute HCl, to give yields of approximately 70%.^[22] The intermediates and the target molecules were characterized by ¹H NMR, ¹³C NMR, and FTIR spectroscopy, MALDI-TOF mass spectrometry, and C, H, N elemental analyses (see Supporting Information). C_n BDKC compounds are readily soluble in CHCl₃, CH₂Cl₂, DMSO, THF, ethyl acetate, and aromatic solvents (such as benzene, toluene, and xylene), whereas they have poor solubility in alcohols (such as methanol and ethanol) and aliphatic hydrocarbon solvents (such as *n*-hexane and *n*-heptane).

Photophysical properties of C_n BDKC in solution: Compounds C1BDKC, C4BDKC, C8BDKC, and C16BDKC possess similar molecular structures except for the length of the alkyl chains, so they give almost the same absorption and emission characteristics in dilute solutions. Therefore, C16BDKC was selected as an example to study their photophysical properties. As shown in Figure 1a, in THF C16BDKC exhibits a broad absorption band at about 300 nm due to the carbazole- and triphenylamine-centered transitions, and two other strong absorption bands at 412 and 432 nm (Table S1, Supporting Information) partly contributed to the charge-transfer (CT) transitions, which can be supported by the solvent-dependent absorption spectra. In hexane, the absorption maximum of C16BDKC is located at 421 nm, which redshifts gradually with increasing polarity of the solvents and reaches 438 nm in acetonitrile (Figure 1, and Figure S22 and Table S1 in the Supporting Information).



Scheme 2. Synthetic routes for the compounds C1BDKC, C4BDKC, C8BDKC, and C16BDKC.

By comparison with the absorption spectral shapes of **C16BDKC** in solvents of different polarity, broadened absorption bands appear in the range of 350–500 nm with a long wavelength tail in more polar solvents, such as acetonitrile, and become structured accompanied by the disappearance of the tail in nonpolar solvents, such as hexane and cyclohexane. These tails seem to originate from the ground-state CT interaction between the donor (triphenylamine) and acceptor (β -diketone) moieties.^[23] On the other hand, it should be noticed that an obvious absorption peak at 350–380 nm can be detected in more polar solvents. We suggest that it might originate from π - π^* transition of C16BDKC, which could be overlapped by the CT band in nonpolar solvents. Upon increasing the polarity of the solvents, the CT band redshifted obviously, which resulted in the emergence of the π - π^* transition band located at 350–380 nm.

Because the CT state is generally sensitive to the exoteric microenvironment, it can be deduced that the fluorescence emission of C16BDKC may be dependent on the solvent. As shown in Figure S23 (Supporting Information), the emission color of C16BDKC in solution can be tuned from blue to yellow with increasing polarity of the solvent. Figure 1b shows the solvent-dependent photoluminescence (PL) spectra of C16BDKC. It is clear that in nonpolar solvents, such as hexane and cyclohexane, the fluorescence spectra of C16BDKC exhibit vibrational structures, which indicates two separated close-lying excited states, so it is deemed that the excited-state contribution to the emission in hexane is the locally excited (LE) one.^[24] The weak solute–solvent interactions in such nonpolar media that do not broaden the vibronic transition too much should be responsible for this

observation. When the polarity of the solvent increases, the fluorescence is structureless and exhibits a solvatochromic redshift due to the dipole–dipole interactions between the solute and solvents.^[25] For example, the fluorescence emission maximum of C16BDKC shows a remarkable redshift of 111 nm from hexane (434 nm) to acetonitrile (545 nm). The maximum of the emission bands shifts significantly to low energy, accompanied by obvious broadening of the emission bands in polar solvents, which indicates an intramolecular charge-transfer (ICT) character for the excited state.^[26] The increase of Stokes shifts with increasing polarity of the solvent pointed to a large solvent relaxation and stronger stabilization of the excited state in polar solvents.^[24a,b] Therefore, it can be expected that an excited

state with a twisted geometry has emerged under excitation of the π -conjugated donor–acceptor system of C16BDKC. Thus, we suggest that C16BDKC gave twisted intramolecular charge-transfer (TICT) emission in polar solvents.

To demonstrate the conformational change of the excited-state surface prior to the emission, we show in Figure 1c a plot of the emission maximum energy as a function of the Lippert solvent polarity.^[27] In such “Lippert–Mataga” plots,^[24c,28] the slope can be used to evaluate the variation in dipole moment upon excitation, and the break in the linear relationship indicates the presence of two different excited states. Accordingly, in the case of C16BDKC, the deviation of the emission maximum energy in hexane and cyclohexane from the linear relationship followed by those in other solvents can further support the notion that the LE state is responsible for the emission in nonpolar solvents and the TICT state contributes to the emission in polar solvents. On the other hand, it is found that C16BDKC is strongly emissive in solvents with medium polarity; for example, the fluorescence quantum yields (Φ_f) of C16BDKC are 0.70 and 0.67 in chloroform and THF, respectively (Table S1, Supporting Information). The lower Φ_f value in more polar solvents (such as 0.17 in acetonitrile) can be attributed to the strong ICT interaction.^[29]

Well-defined nanowires based on C1BDKC: Generally, if π -stacking interaction between the molecules with extended π -conjugated units is predominant over the lateral association caused by the hydrophobic interaction among the side chains, the functional molecules would prefer to arrange

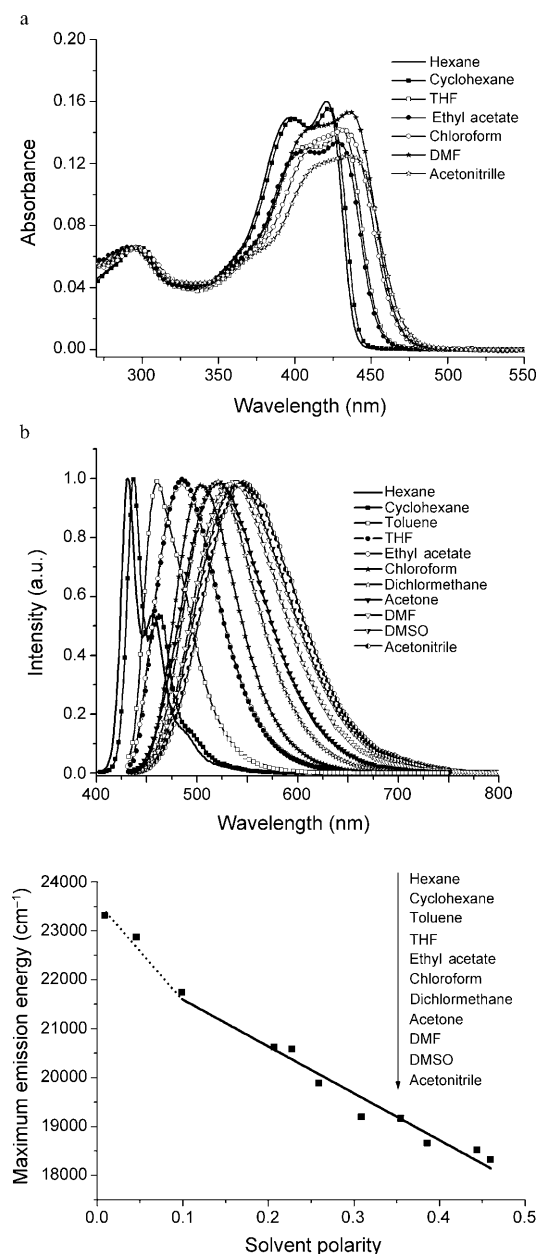


Figure 1. a) Normalized UV/Vis absorption and b) PL spectra of C1BDKC in different solvents (2.0×10^{-6} M). c) Lippert–Mataga plot: fluorescence emission maximum energy of C1BDKC as a function of solvent polarity.

along the stacking axis into 1D nanostructures.^[2a] In our case, only a short alkyl chain (methyl) is connected to the 9-position of carbazole in C1BDKC, which means that C1BDKC would like to form 1D self-assemblies through strong π - π stacking. As anticipated, 1D nanowires based on C1BDKC were expediently fabricated by the reprecipitation approach.^[2,30] As shown in Figure 2a–c, the scanning electron microscopy (SEM) and transmission electron microscopy (TEM) images of the self-assemblies of C1BDKC reveal well-defined 1D straight nanowires with high aspect ratio, for example, a length of hundreds of micrometers and width

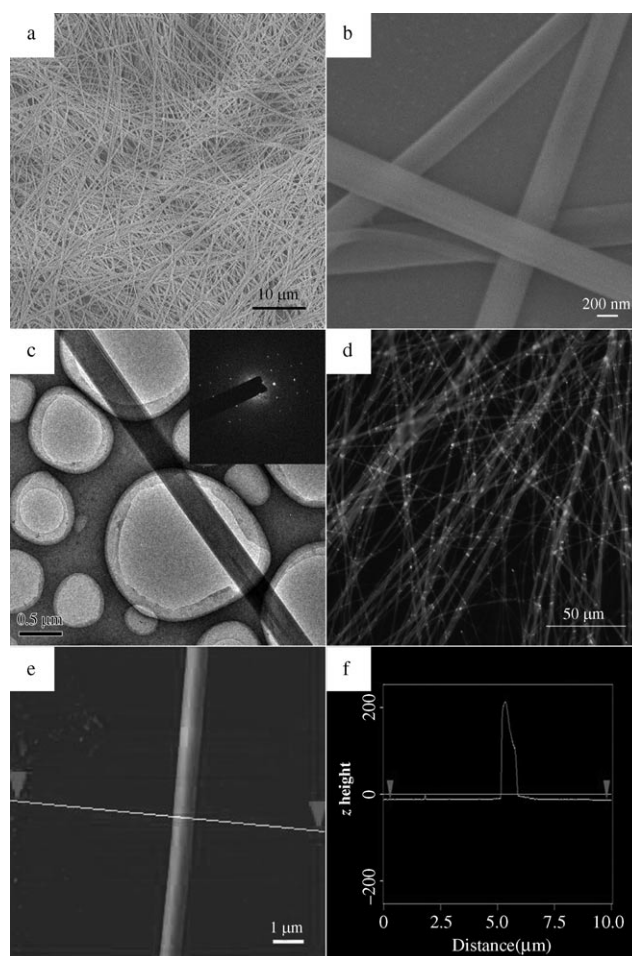


Figure 2. a, b) SEM, c) TEM, d) fluorescence microscopy, and e) AFM images of C1BDKC-based nanowires obtained by the reprecipitation approach; f) line-scan profile (marked in (e)). Note that due to the diffraction effect of the nanowires, their diameter in the optical microscopy image appears larger than the real size as measured by SEM and TEM. The inset in (c) depicts the electronic diffraction pattern. The excitation wavelength for fluorescence microscopy measurements was 330–385 nm.

of 200–1000 nm. From the atomic force microscopy (AFM) image as shown in Figure 2e, we can also find well-defined nanowires, similar to those observed in the SEM and TEM images. Furthermore, the line-scan profile suggests the aspect ratio of the cross section (width/thickness) of the nanowire is around 4:1 (Figure 2f and Figure S24a,b in the Supporting Information).^[10e,11a] Notably, the appearance of sharp diffraction spots in the electron diffraction pattern of the nanowires (inset of Figure 2c) and the sharp diffraction peaks in the wide-angle X-ray diffraction pattern (Figure 3a) illustrate that C1BDKC molecules pack into highly ordered arrays in the nanowires. For instance, the diffraction peak with a d -spacing of 0.42 nm is close to a typical π - π stacking distance (0.35 nm), suggesting that π - π interaction is the main driving force for the formation of nanowires, which can be further confirmed by the significant redshift of the absorption of C1BDKC-based nanowires compared with that in solution (see below). The other two sharp diffrac-

tions correspond to the peaks with d -spacings of 1.32 and 0.45 nm, close to a ratio of 1:1/3. Therefore, we can deduce a lamellar organization in the aggregates of C1BDKC with an interlayer distance of 1.32 nm.^[31] In addition, semiempirical (AM1) calculations have been performed to optimize the ground-state geometry of C1BDKC to help us to understand the molecular packing model in the nanowires. The molecular width is estimated to be 1.32 nm (Figure 3b), which is in accordance with the period of the lamellar structure in the crystal state based on XRD data.

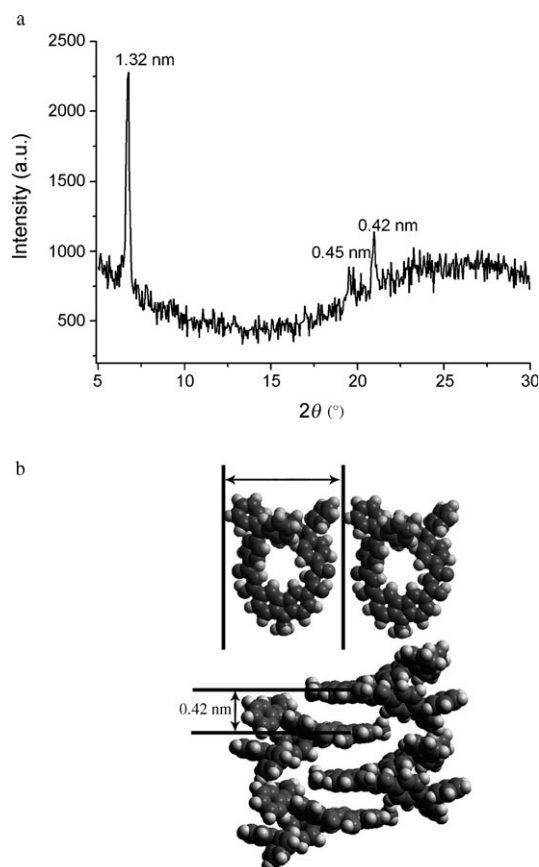


Figure 3. a) X-ray diffraction pattern of nanowires of C1BDKC deposited on glass. b) Proposed molecular packing model of C1BDKC in nanowires.

On the other hand, as shown in Figure 4, the absorption bands of the nanowires became broad and the maximum redshifted significantly to 455 nm compared with that in hexane (421 nm), which indicated the formation of J-aggregates in the nanowires. Thus, we can deduce that C1BDKC molecules are arranged in parallel along the growth direction of the wire and are further extended to form a 1D structure. The molecular packing model is proposed in Figure 3b, in which the distance between two parallel bis(β -diketone)carbazole moieties is 0.42 nm, which matched the XRD result. Notably, the C1BDKC-based nanowires can emit strong green light under irradiation at 330–385 nm, as

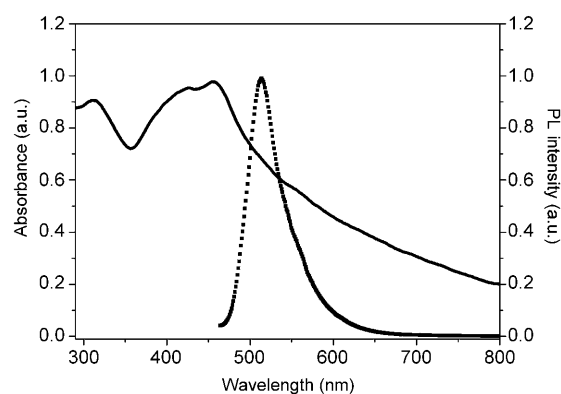


Figure 4. Normalized UV/Vis absorption (—) and fluorescence (-----, $\lambda_{\text{ex}} = 460$ nm) spectra of C1BDKC-based nanowires deposited on a quartz slide. The raised baseline for the absorption spectrum of the nanowire film is primarily due to light scattering.

shown by the fluorescence microscopy image (Figure 2d and Figure S24c in the Supporting Information). The fluorescence emission spectrum of C1BDKC-based nanowires is given in Figure 4; the emission of the nanowires appears at 513 nm, which shows a redshift of approximately 89 nm relative to that in hexane. It further indicates that the aromatic π stacking plays a key role in the self-assembly of C1BDKC. In addition, from the fluorescence decay profiles of C1BDKC in nanowires and in hexane solution (5.0×10^{-6} M), we obtained lifetimes of 0.99 and 1.06 ns for the nanowires and monomeric species, respectively (Figure S25). The shorter fluorescence lifetime of C1BDKC in nanowires relative to that in dilute solution further confirmed the formation of J-aggregates in nanowires.^[32] As a result, the C1BDKC-based nanowires with strong emission may find potential applications in emitting materials as well as optical devices.

Organogel fibers based on C16BDKC: As discussed above, C1BDKC with a short methyl chain prefers to self-assemble into nanowires through strong π - π interaction. For comparison, we synthesized three other C_n BDKC compounds with butyl (C4BDKC), octyl (C8BDKC), and hexadecyl (C16BDKC) groups. As for compounds C4BDKC and C8BDKC, only ill-defined agglomerates, rather than 1D nanostructures, are obtained by the reprecipitation approach. The reason might be that the π - π interaction is disturbed by the interaction between the side chains, which is, however, not strong enough to dominate the self-assembly process. Nevertheless, when the side chain is lengthened to hexadecyl, van der Waals interaction between the long alkyl groups would cooperate with π - π interaction between the conjugated units, and might lead to self-assembly behavior of C16BDKC different from that of the other C_n BDKC compounds. Fortunately, 1D nanofibers based on C16BDKC can be easily generated by organogelation in cyclohexane, 1-hexanol, toluene/hexane (1:4, v/v), toluene/heptane (1:5, v/v) etc. under ultrasound stimulation instead of a heating-cooling process (Table S2, Supporting Information), because the precipitates are obtained from the above solvents after

cooling the hot solution of C16BDKC to room temperature followed by aging for 1 h. The critical gelation concentration (CGC) varied in the range of 1.8–2.2 mM depending on the solvent. In addition, the obtained C16BDKC-based gels were stable, and could not be destroyed after several months at room temperature. To obtain the morphology of the self-assemblies of C16BDKC in the gel state, SEM, TEM, and AFM measurements were performed. The SEM and TEM images of the xerogels obtained from cyclohexane show lots of entangled 1D nanofibers around 100 nm in diameter (Figure 5 a–c and Figure S26a in the Supporting In-

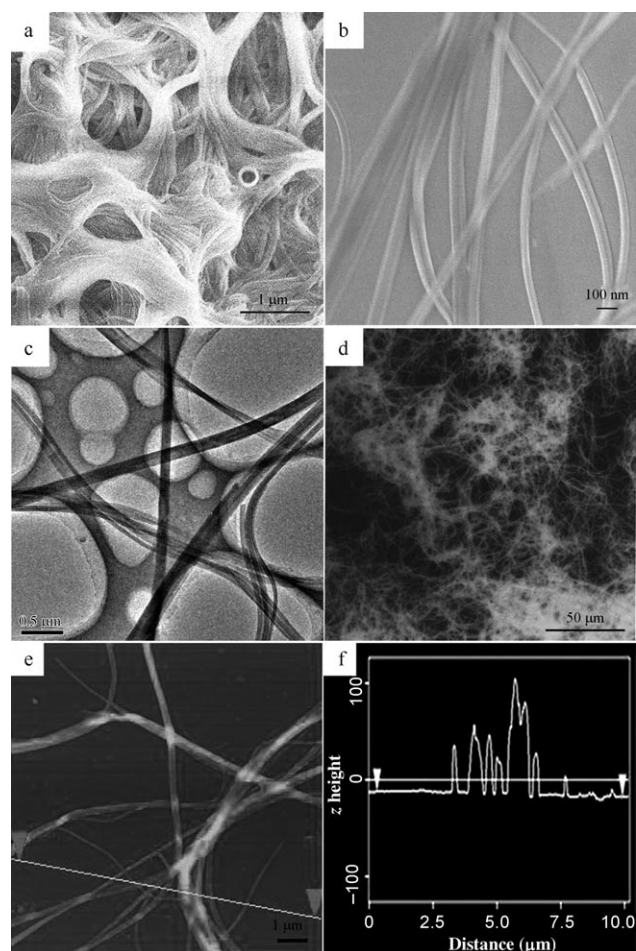


Figure 5. a, b) SEM, c) TEM, d) fluorescence microscopy, and e) AFM images of the C16BDKC gel obtained from cyclohexane; f) z-height line-scan profile over the fibers marked in (e). The excitation wavelength for fluorescence microscopy measurements was 330–385 nm.

formation). Similarly, AFM images of the cyclohexane gel shown in Figure 5e and f also illustrate that the intertwined fiber bundles are built up from thin fibrils around 100 nm in width and several micrometers in length. The fluorescence microscopy image (Figure 5d and Figure S26b) illustrates that the C16BDKC-based nanofibers emit strong green light in the gel phase.

To obtain information on the organization of chromophores in the gel state, time-dependent UV/Vis spectra of C16BDKC were measured in cyclohexane (2.0×10^{-3} M) by ultrasound treatment followed by aging for a certain time (Figure 6a). After a brief sonication, the solution of

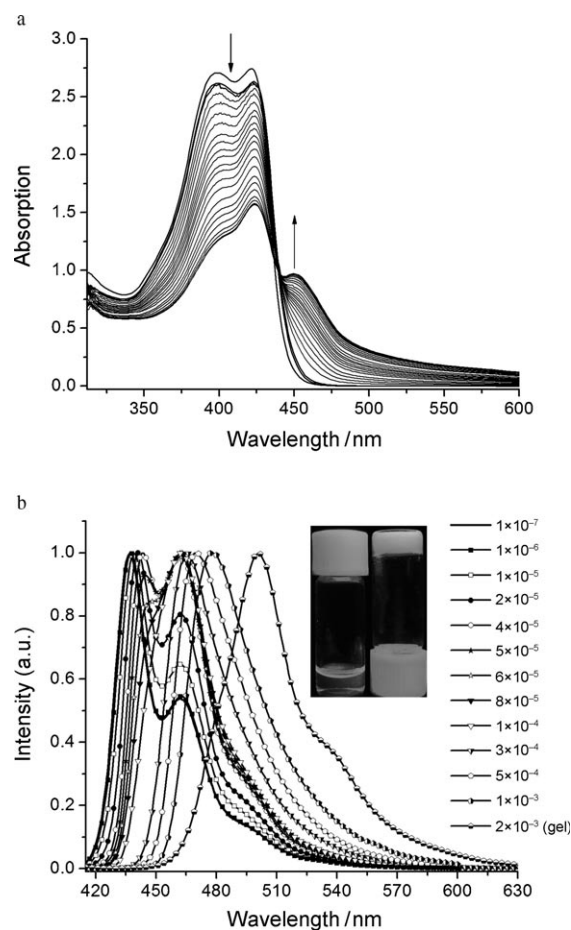


Figure 6. a) Time-dependent UV/Vis spectra of C16BDKC in cyclohexane at 2.0×10^{-3} M with ultrasound treatment followed by aging for a certain time (the interval is 40 s). b) Normalized concentration-dependent fluorescence spectra of C16BDKC in cyclohexane solution and in the gel state at 25 °C ($\lambda_{\text{ex}} = 415$ nm). Inset: photographs of C16BDKC (2.0×10^{-3} M) dissolved in cyclohexane at 70 °C (left vial) and the corresponding organogel at 25 °C (right vial) under irradiation at 365 nm.

C16BDKC begins to transform into a gel. The absorption band at 422 nm does not shift, but its intensity decreases gradually during the gelation process. Additionally, a new absorption peak located at 450 nm appears upon gel formation, and increases gradually with time. The findings indicate that π - π interaction plays a key role in gel formation.^[33] Meanwhile, the fluorescence spectra of C16BDKC in cyclohexane at different concentrations as well as in the gel state at 25 °C are given in Figure 6b. In dilute solution (1.0×10^{-7} – 6.0×10^{-5} M), two emission bands at about 440 and 460 nm were detected, and the ratio of the emission intensity of the two peaks became smaller gradually with increasing concentration. When the concentration reached 8.0×10^{-5} M, the

former peak became a shoulder of the one at about 460 nm. As the concentration was further increased, the emission redshifted significantly to 478 nm at 1.0×10^{-3} M due to molecular aggregation. In the gel state, the emission peak of C16BDKC emerged at 501 nm with a weak shoulder around 540 nm, which suggested the formation of π aggregates in the gel phase. Moreover, we deem that H-aggregates are formed from C16BDKC in the gel phase according to the following evidence. Firstly, the fluorescence decay profile for C16BDKC-based gel in cyclohexane (2.0×10^{-3} M, Figure S27) reveals that the fluorescence lifetime of C16BDKC in the gel phase is 1.76 ns, which is longer than that in cyclohexane solution at 1.0×10^{-5} M (1.09 ns). It is one piece of evidence to testify the formation of H-aggregates.^[34] Secondly, the excitation spectrum of C16BDKC-based gel (Figure S28) does not correspond in shape or position to its absorption spectrum: two bands at 342 and 465 nm appeared in the excitation spectrum, while the absorption bands were located at 422 and 450 nm. These results provide further proof for the “trapping” or localization of excitation in H-aggregates.^[35] Finally, the decreased fluorescence emission intensity of C16BDKC in the gel state relative to that in solution (Figure S29) is also consistent with the formation of H-aggregates.^[36] Although the formed H-aggregates would induce a decrease of the emission intensity, the gel can still emit strong green light (inset of Figure 6b and Figure S26b in the Supporting Information), which makes C16BDKC-based nanofibers a good candidate for emitting materials.

The vibration frequencies for CH_2 , including antisymmetric $\nu_{\text{as}}(\text{CH}_2)$ and symmetric $\nu_{\text{s}}(\text{CH}_2)$ stretching, in the xerogel could somewhat reflect the packing conformation of alkyl chains,^[7c,37] and therefore the FTIR spectrum of the xerogel of C16BDKC is shown in Figure S30 (Supporting Information). The $\nu_{\text{as}}(\text{CH}_2)$ and $\nu_{\text{s}}(\text{CH}_2)$ bands appear at 2920 and 2850 cm^{-1} , respectively, in a relatively low wavenumber region, thus suggesting that the alkyl chains adopted an all-*trans* conformation. Thus, the cooperation of van der Waals and aromatic π -stacking interactions is critical for gel formation from C16BDKC. The XRD pattern of the xerogel of C16BDKC obtained from cyclohexane shows a series of sharp diffraction peaks (Figure S31). The strongest peak at $2\theta = 6.80^\circ$ corresponded to a *d*-spacing of 1.30 nm, which was close to the width of the molecule (Figure S32). Although it is difficult to propose the molecular packing model in the self-assemblies of C16BDKC from XRD results, the observed diffraction pattern suggests the ordered arrangement of C16BDKC in the gel state to some extent.^[38]

Conclusion

A series of new triphenylamine-functionalized bis(β -diketone)s bridged by carbazole (*C_n*BDKC, *n* = 1, 4, 8, 16) with alkyl chains of different length have been synthesized. Such donor–acceptor-type π -conjugated molecules give CT transitions in the ground state and TICT emission in polar sol-

vents, so they can be used as TICT probes to sense the changes of the external environment. It should be noted that the length of the carbon chains plays a key role in the self-assembling properties of *C_n*BDKC. For example, well-defined nanowires could be easily fabricated from C1BDKC with a short methyl side chain by a reprecipitation approach, and π -stacking interaction is confirmed as the main driving force for the formation of nanowires, in which C1BDKC packed into J-aggregates. Meanwhile, C16BDKC bearing a long hexadecyl chain can self-assemble into an organogel under ultrasound stimulation and lots of 1D nanofibers are observed in the gel phase. However, H-aggregates are formed through cooperation of π -stacking and van der Waals interactions in the gel phase. In the cases of C4BDKC and C8BDKC containing butyl and octyl groups, respectively, only ill-defined agglomerates rather than 1D nanostructures are obtained. The reason might be that π - π interaction might be disturbed by the interaction between the side chains, which is, however, not strong enough to dominate the self-assembly process. Notably, the generated 1D nanowires based on C1BDKC and nanofibers from C16BDKC can emit strong green light under irradiation, which suggests that these 1D nanomaterials may have potential applications in emitting materials as well as photonic devices.

Experimental Section

Measurement and characterization: ^1H and ^{13}C NMR spectra were recorded with a Mercury Plus instrument at 500 and 125 MHz by using CDCl_3 as the solvent in all cases. IR spectra were measured with a Nicolet-360 FTIR spectrometer by incorporation of samples in KBr disks. UV/Vis spectra were determined with a Shimadzu UV-1601PC spectrophotometer. PL spectra were recorded with a Shimadzu RF-5301 luminescence spectrometer. Fluorescence lifetimes were measured by using the time-correlated single photon counting technique with an FL920 fluorescence lifetime spectrometer. The excitation source was an nF900 nanosecond flashlamp. Lifetimes were obtained by deconvolution of the decay curves. Mass spectra were obtained with Agilent 1100 MS series and AXIMA CFR MALDI-TOF (Compact) mass spectrometers. C, H, and N elemental analyses were performed with a Perkin–Elmer 240C elemental analyzer. SEM was performed on a JEOL JSM-6700F instrument (operating at 5 kV). The sample was prepared by casting the nanowire suspension in hexane or gel onto a clean silicon wafer followed by drying in air. The dried sample was then annealed overnight in an oven at 45 °C, followed by coating of gold. TEM experiments were performed by using a JEM 3010 electron microscope (JEOL, Japan) with an acceleration voltage of 300 kV. The samples for TEM measurement were prepared by wiping a small amount of nanowires or gel onto a 300-mesh copper grid followed by natural evaporation of the solvent. AFM measurement was carried out with a commercial instrument (Digital Instruments, Dimension 3100, Santa Barbara, CA) running in tapping mode. Si cantilevers (Nanosensors) with resonance frequencies of 250–350 kHz were used. The samples were prepared by drop-casting the nanowire suspension in hexane or gel onto a silicon wafer then evaporating the solvent slowly at room temperature under vacuum. Fluorescence microscopy images were taken on a fluorescence microscope (Olympus Reflected Fluorescence System BX51, Olympus, Japan). The samples were prepared by casting the nanowire suspension in hexane or gel on a glass slide and drying at room temperature. XRD patterns were obtained on a Japan Rigaku D/max- γ A instrument equipped with graphite-monochromatized $\text{Cu}_{\text{K}\alpha}$ radiation ($\lambda = 1.5418 \text{ \AA}$), by employing a scanning rate of $0.02^\circ \text{ s}^{-1}$ in the 2θ

range from 0.7 to 10°, and 0.05° s⁻¹ in the 2θ range from 10 to 30°. The samples were prepared by casting the nanowires or gels on glass slides and drying at room temperature.

Fabrication of nanowires: C1BDKC-based nanowires were prepared by the reprecipitation method. Typically, a concentrated chloroform solution of C1BDKC (0.2 mL, 1.0 mm) was injected rapidly into hexane (10 mL) with sufficient stirring followed by aging for 2 days at room temperature, and then nanowires in the form of yellow aggregates were formed. The aged aqueous suspension of the nanowires was transferred onto a quartz slide followed by drying in air for spectroscopic measurements.

Preparation of C16BDKC-based gels: A clear solution of C16BDKC was obtained by heating. The gel was formed after the hot solution was sonicated for 10 min followed by aging for 1 h at room temperature.

Synthesis: THF was freshly distilled from sodium and benzophenone. CH₂Cl₂ was distilled from CaH₂. The other chemicals and reagents were used as received from commercial sources without further purification. Compounds 1–6 and methyl 4-(diphenylamino)benzoate were synthesized according to the literature.^[20,21,39–41]

9-*n*-Hexadecylcarbazole (4): NaH (60%, 2.1 g, 52.0 mmol) and *n*-C₁₆H₃₃Br (10.0 g, 32.8 mmol) were added to a solution of carbazole (5.0 g, 29.9 mmol) in DMF (60 mL). The mixture was stirred at room temperature until the disappearance of carbazole (monitored by TLC). The mixture was poured into water (500 mL) and the precipitate was collected by filtration. The solid was recrystallized from ethanol to give a white solid (10.6 g). Yield 90%; m.p. 54.0–56.0°C; ¹H NMR (500 MHz, TMS, CDCl₃): δ = 8.09 (d, *J* = 7.5 Hz, 2H), 7.45 (t, *J* = 7.5, 7.5 Hz, 2H), 7.39 (d, *J* = 8.0 Hz, 2H), 7.21 (t, *J* = 5.5, 9.0 Hz, 2H), 4.27 (t, *J* = 7.5, 7.0 Hz, 2H), 1.88–1.82 (m, 2H), 1.38–1.23 (m, 26H), 0.88 ppm (t, *J* = 6.5 Hz, 3H); ¹³C NMR (125 MHz, CDCl₃): δ = 140.9, 126.0, 123.3, 120.8, 119.1, 109.1, 68.4, 43.5, 32.4, 30.1, 30.0, 29.9, 29.4, 27.8, 26.1, 23.2, 14.6 ppm; IR (KBr): $\tilde{\nu}$ = 719, 746, 1122, 1151, 1228, 1325, 1350, 1396, 1466, 1485, 1508, 1541, 1560, 1593, 1655, 1670, 1685, 1718, 2848, 2920 cm⁻¹; MALDI-TOF MS: *m/z*: calcd for C₂₈H₄₁N: 391.6; found: 391.5; elemental analysis (%) calcd for C₂₈H₄₁N: C 85.87, H 10.55, N, 3.58; found: C 85.56, H 10.67, N, 3.65.

3,6-Diacetyl-9-(*n*-octyl)-carbazole (7): Acetyl chloride (7.2 g, 91.8 mmol) was added slowly over 30 min to a suspension of AlCl₃ (12.2 g, 91.8 mmol) in 1,2-dichloroethane (100 mL) at 5°C. Compound 3 (10.7 g, 38.3 mmol) was then added slowly, and the reaction mixture was stirred for 2 h at room temperature and then for 2 h at 35°C. After cooling, the solvent was removed under reduced pressure. Dilute HCl (200 mL) was added to the flask and a white solid appeared. The solid was collected by filtration and washed with water, followed by recrystallization from ethanol to give a white solid (12.0 g). Yield 86%; m.p. 90.0–92.0°C; ¹H NMR (500 MHz, TMS, CDCl₃): δ = 8.75 (s, 2H), 8.16 (d, *J* = 8.5 Hz, 2H), 7.42 (d, *J* = 8.5 Hz, 2H), 4.31 (t, *J* = 6.0, 7.0 Hz, 2H), 2.73 (s, 6H), 1.90–1.84 (m, 2H), 1.38–1.20 (m, 10H), 0.85 ppm (t, *J* = 7.0, 7.0 Hz, 3H); ¹³C NMR (125 MHz, CDCl₃): δ = 197.8, 144.3, 130.1, 127.4, 123.3, 122.4, 109.4, 44.0, 32.1, 29.7, 29.5, 29.3, 27.6, 27.0, 23.0, 14.4 ppm; IR (KBr): $\tilde{\nu}$ = 621, 669, 721, 814, 901, 957, 1026, 1072, 1130, 1254, 1306, 1367, 1468, 1491, 1570, 1593, 1672, 2848, 2920 cm⁻¹; MALDI-TOF MS: *m/z*: calcd for C₂₄H₂₉NO₂: 363.5; found: 363.9; elemental analysis (%) calcd for C₂₄H₂₉NO₂: C 79.30, H 8.04, N 3.85; found: C 79.02, H 7.96, N 3.79.

3,6-Diacetyl-9-(*n*-hexadecyl)-carbazole (8): By following the synthetic procedure for compound 7, compound 8 (11.0 g) was synthesized with acetyl chloride (4.8 g, 61.2 mmol), AlCl₃ (8.2 g, 61.2 mmol), compound 4 (10.0 g, 25.5 mmol), and 1,2-dichloroethane (100 mL) as reagents. Yield 91%; m.p. 111.0–113.0°C; ¹H NMR (500 MHz, TMS, CDCl₃): δ = 8.75 (s, 2H), 8.15 (d, *J* = 8.5 Hz, 2H), 7.42 (d, *J* = 8.5 Hz, 2H), 4.29 (t, *J* = 6.5, 6.5 Hz, 2H), 2.73 (s, 6H), 1.89–1.84 (m, 2H), 1.36–1.22 (m, 26H), 0.87 ppm (t, *J* = 7.0, 7.0 Hz, 3H); ¹³C NMR (125 MHz, CDCl₃): δ = 197.7, 144.2, 130.1, 127.3, 123.2, 122.3, 109.3, 68.3, 44.0, 32.3, 30.1, 30.0, 29.9, 29.8, 29.7, 29.6, 29.3, 27.6, 27.4, 27.0, 26.8, 26.0, 23.1, 14.5 ppm; IR (KBr): $\tilde{\nu}$ = 621, 669, 721, 814, 903, 953, 1026, 1072, 1130, 1265, 1306, 1365, 1468, 1491, 1570, 1595, 1674, 2848, 2919 cm⁻¹; MALDI-TOF MS: *m/z*: calcd for C₃₂H₄₅NO₂: 475.7; found: 476.4; elemental analysis (%) calcd for C₃₂H₄₅NO₂: C 80.79, H 9.53, N 2.94; found: C 80.68, H 9.42, N 2.70.

3,6-Di(3-[1-[4-(diphenylamino)phenyl]-1,3-dioxopropyl])-9-methylcarbazole (C1BDKC): Sodium hydride (60%, 1.00 g, 25.00 mmol) was added

quickly to a solution of compound 5 (1.00 g, 3.77 mmol) and methyl 4-(diphenylamino)benzoate (2.80 g, 9.24 mmol) in THF (60 mL). The reaction mixture was heated under an atmosphere of nitrogen at 60°C for 24 h, and then cooled to room temperature. The mixture was acidified with dilute HCl and extracted with CH₂Cl₂. After solvent removal, the solid residue was purified by column chromatography (silica gel; CH₂Cl₂) to give a yellow solid (2.28 g). Yield 75%; m.p. 258.0–260.0°C; ¹H NMR (500 MHz, TMS, CDCl₃): δ = 8.75 (s, 2H), 8.12 (d, *J* = 8.5 Hz, 2H), 7.88 (d, *J* = 8.5 Hz, 4H), 7.41 (d, *J* = 8.5 Hz, 2H), 7.32 (t, *J* = 7.5, 8.0 Hz, 8H), 7.19–7.12 (m, 12H), 7.07 (d, *J* = 8.5 Hz, 4H), 6.88 (s, 2H), 3.87 ppm (s, 3H); ¹³C NMR (125 MHz, CDCl₃): δ = 185.8, 184.4, 152.0, 147.1, 144.3, 130.0, 128.9, 128.3, 128.1, 126.2, 124.9, 123.4, 120.9, 120.7, 109.2, 92.2, 30.0 ppm; IR (KBr): $\tilde{\nu}$ = 669, 694, 752, 785, 1120, 1170, 1220, 1260, 1400, 1440, 1460, 1490, 1580, 1590, 1620, 2850, 2930 cm⁻¹; MALDI-TOF MS: *m/z*: calcd for C₅₅H₄₁N₃O₄: 807.9; found: 808.7; elemental analysis (%) calcd for C₅₅H₄₁N₃O₄: C 81.76, H 5.11, N 5.20; found: C 81.65, H 5.21, N 5.11.

3,6-Di(3-[1-[4-(diphenylamino)phenyl]-1,3-dioxopropyl])-9-(*n*-butyl)-carbazole (C4BDKC): By following the synthetic procedure for C1BDKC, C4BDKC was synthesized with compound 6 (1.10 g, 3.58 mmol), methyl 4-(diphenylamino)benzoate (2.61 g, 8.60 mmol), and sodium hydride (60%, 1.00 g, 25.00 mmol) as reagents. The crude product was purified by column chromatography (silica gel; petroleum ether/CH₂Cl₂, 1:5 v/v) to give a yellow solid (2.20 g). Yield 72%; m.p. 154.0–156.0°C; ¹H NMR (500 MHz, TMS, CDCl₃): δ = 8.77 (s, 2H), 8.11 (d, *J* = 8.5 Hz, 2H), 7.89 (d, *J* = 8.5 Hz, 4H), 7.43 (d, *J* = 8.5 Hz, 2H), 7.32 (t, *J* = 8.0, 7.5 Hz, 8H), 7.18–7.12 (m, 12H), 7.07 (d, *J* = 9.0 Hz, 4H), 6.89 (s, 2H), 4.31 (t, *J* = 7.0, 7.0 Hz, 2H), 1.90–1.84 (m, 2H), 1.44–1.36 (m, 2H), 0.96 ppm (t, *J* = 7.5, 7.5 Hz, 3H); ¹³C NMR (125 MHz, CDCl₃): δ = 185.8, 184.4, 152.0, 147.1, 143.9, 130.0, 128.9, 128.3, 126.2, 126.0, 124.9, 123.5, 120.9, 120.7, 109.5, 92.2, 43.8, 31.5, 20.9, 14.2 ppm; IR (KBr): $\tilde{\nu}$ = 621, 696, 752, 783, 1110, 1180, 1210, 1270, 1380, 1460, 1490, 1590, 2850, 2920 cm⁻¹; MALDI-TOF MS: *m/z*: calcd for C₃₈H₄₇N₃O₄: 850.0; found: 850.3; elemental analysis (%) calcd for C₃₈H₄₇N₃O₄: C 81.95, H 5.57, N 4.94; found: C 81.83, H 5.68, N 4.72.

3,6-Di(3-[1-[4-(diphenylamino)phenyl]-1,3-dioxopropyl])-9-(*n*-octyl)-carbazole (C8BDKC): By following the synthetic procedure for C1BDKC, C8BDKC was synthesized with compound 7 (1.8 g, 4.95 mmol), methyl 4-(diphenylamino)benzoate (3.76 g, 12.38 mmol), and sodium hydride (60%, 1.41 g, 35.34 mmol) as reagents. The crude product was purified by column chromatography (silica gel; petroleum ether/CH₂Cl₂, 2:3 v/v) to give a yellow solid (3.14 g). Yield 70%; m.p. 128.0–130.0°C; ¹H NMR (500 MHz, TMS, CDCl₃): δ = 8.79 (s, 2H), 8.13 (d, *J* = 8.5 Hz, 2H), 7.91 (d, *J* = 9.0 Hz, 4H), 7.44 (d, *J* = 8.5 Hz, 2H), 7.34 (t, *J* = 8.0, 7.5 Hz, 8H), 7.21–7.14 (m, 12H), 7.10 (d, *J* = 8.5 Hz, 4H), 6.91 (s, 2H), 4.31 (d, *J* = 5.5 Hz, 2H), 1.93–1.86 (m, 2H), 1.39–1.25 (m, 10H), 0.88 ppm (t, *J* = 8.5, 7.5 Hz, 3H); ¹³C NMR (125 MHz, CDCl₃): δ = 185.9, 184.4, 152.0, 147.1, 143.9, 128.9, 128.3, 128.1, 126.2, 126.1, 124.9, 123.5, 120.9, 120.8, 109.5, 92.2, 44.0, 32.2, 29.7, 29.5, 29.4, 27.6, 23.0, 14.5 ppm; IR (KBr): $\tilde{\nu}$ = 619, 698, 754, 783, 1120, 1180, 1220, 1270, 1380, 1460, 1490, 1590, 2850, 2920 cm⁻¹; MALDI-TOF MS: *m/z*: calcd for C₆₂H₅₅N₃O₄: 906.1; found: 907.0; elemental analysis (%) calcd for C₆₂H₅₅N₃O₄: C 82.18, H 6.12, N 4.64; found: C 82.09, H 5.94, N 4.56.

3,6-Di(3-[1-[4-(diphenylamino)phenyl]-1,3-dioxopropyl])-9-(*n*-hexadecyl)-carbazole (C16BDKC): By following the synthetic procedure for C1BDKC, C16BDKC was synthesized with compound 8 (2.00 g, 4.20 mmol), methyl 4-(diphenylamino)benzoate (3.20 g, 10.55 mmol), and sodium hydride (60%, 1.20 g, 30.00 mmol) as reagents. The crude product was purified by column chromatography (silica gel; petroleum ether/CH₂Cl₂, 2:3 v/v) to give a yellow solid (2.85 g). Yield 67%; m.p. 164.0–166.0°C; ¹H NMR (500 MHz, TMS, CDCl₃): δ = 8.72 (s, 2H), 8.08 (d, *J* = 8.0 Hz, 2H), 7.88 (d, *J* = 8.5 Hz, 4H), 7.38 (d, *J* = 8.0 Hz, 2H), 7.31 (t, *J* = 8.0, 7.5 Hz, 8H), 7.18–7.11 (m, 12H), 7.06 (d, *J* = 9.0 Hz, 4H), 6.86 (s, 2H), 4.26 (s, 2H), 1.85 (s, 2H), 1.32–1.21 (m, 26H), 0.86 ppm (t, *J* = 4.5, 6.5 Hz, 3H); ¹³C NMR (125 MHz, CDCl₃): δ = 185.8, 184.3, 152.0, 147.1, 143.8, 130.0, 128.9, 128.3, 128.0, 126.2, 126.0, 124.9, 123.5, 120.9, 120.7, 109.5, 92.2, 68.4, 51.0, 44.0, 32.4, 30.1, 30.0, 29.9, 29.8, 29.4, 27.7, 26.1, 23.1, 14.6 ppm; IR (KBr): $\tilde{\nu}$ = 621, 692, 750, 783, 1120, 1180, 1220, 1270,

1380, 1460, 1490, 1590, 2850, 2920 cm⁻¹; MALDI-TOF MS: *m/z*: calcd for C₇₀H₇₁N₃O₄: 1018.3; found: 1018.7; elemental analysis (%) calcd for C₇₀H₇₁N₃O₄: C 82.56, H 7.03, N 4.13; found: C 82.38, H 6.86, N 3.98.

Acknowledgements

This work was financially supported by the National Natural Science Foundation of China (NNSFC, No. 20874034), the 973 Program (2009CB939701), and the Open Project of State Key Laboratory of Supramolecular Structure and Materials (SKLSSM200901).

- [1] a) F. J. M. Hoeben, P. Jonkheijm, E. W. Meijer, A. P. H. J. Schenning, *Chem. Rev.* **2005**, *105*, 1491–1546; b) A. Ajayaghosh, V. K. Praveen, *Acc. Chem. Res.* **2007**, *40*, 644–656.
- [2] a) L. Zang, Y. Che, J. S. Moore, *Acc. Chem. Res.* **2008**, *41*, 1596–1608; b) Y. Zhao, H. Fu, A. Peng, Y. Ma, Q. Liao, J. Yao, *Acc. Chem. Res.* **2010**, *43*, 409–418.
- [3] a) A. P. H. J. Schenning, E. W. Meijer, *Chem. Commun.* **2005**, 3245–3258; b) A. Ajayaghosh, S. J. George, *J. Am. Chem. Soc.* **2001**, *123*, 5148–5149; c) H. Liu, Y. Li, S. Xiao, H. Gan, T. Jiu, H. Li, L. Jiang, D. Zhu, D. Yu, B. Xiang, Y. Chen, *J. Am. Chem. Soc.* **2003**, *125*, 10794–10795; d) D. T. Bong, T. D. Clark, J. R. Granja, M. R. Ghadiri, *Angew. Chem.* **2001**, *113*, 1016–1041; *Angew. Chem. Int. Ed.* **2001**, *40*, 988–1011.
- [4] a) B. K. An, S. K. Kwon, S. Y. Park, *Angew. Chem.* **2007**, *119*, 2024–2028; *Angew. Chem. Int. Ed.* **2007**, *46*, 1978–1982; b) S. J. Lim, B. K. An, S. D. Jung, M. A. Chung, S. Y. Park, *Angew. Chem.* **2004**, *116*, 6506–6510; *Angew. Chem. Int. Ed.* **2004**, *43*, 6346–6350; c) B. K. An, S. K. Kwon, S. D. Jung, S. Y. Park, *J. Am. Chem. Soc.* **2002**, *124*, 14410–14415.
- [5] a) A. Peng, D. Xiao, Y. Ma, W. Yang, J. Yao, *Adv. Mater.* **2005**, *17*, 2070–2073; b) D. Xiao, L. Xi, W. Yang, H. Fu, Z. Shuai, Y. Fang, J. Yao, *J. Am. Chem. Soc.* **2003**, *125*, 6740–6745; c) H. Fu, B. H. Loo, D. Xiao, R. Xie, X. Ji, J. Yao, B. Zhang, L. Zhang, *Angew. Chem.* **2002**, *114*, 1004–1007; *Angew. Chem. Int. Ed.* **2002**, *41*, 962–965.
- [6] a) Y. Liu, H. Li, D. Tu, Z. Ji, C. Wang, Q. Tang, M. Liu, W. Hu, Y. Liu, D. Zhu, *J. Am. Chem. Soc.* **2006**, *128*, 12917–12922; b) J. K. Lee, W. K. Koh, W. S. Chae, Y. R. Kim, *Chem. Commun.* **2002**, 138–139; c) J. S. Hu, Y. G. Guo, H. P. Liang, L. J. Wan, L. Jiang, *J. Am. Chem. Soc.* **2005**, *127*, 17090–17095; d) C. Wang, Q. Chen, F. Sun, D. Zhang, G. Zhang, Y. Huang, R. Zhang, D. Zhu, *J. Am. Chem. Soc.* **2010**, *132*, 3092–3096.
- [7] a) C. Y. Bao, R. Lu, M. Jin, P. C. Xue, C. H. Tan, G. F. Liu, Y. Y. Zhao, *Org. Biomol. Chem.* **2005**, *3*, 2508–2512; b) P. C. Xue, R. Lu, G. J. Chen, Y. Zhang, H. Nomoto, M. Takafuji, H. Ihara, *Chem. Eur. J.* **2007**, *13*, 8231–8239; c) C. Y. Bao, R. Lu, M. Jin, P. C. Xue, C. H. Tan, T. H. Xu, G. F. Liu, Y. Y. Zhao, *Chem. Eur. J.* **2006**, *12*, 3287–3294; d) X. C. Yang, R. Lu, T. H. Xu, P. C. Xue, X. L. Liu, ; Y. Y. Zhao, *Chem. Commun.* **2008**, 453–455; Y. Y. Zhao, *Chem. Commun.* **2008**, 453–455; e) X. C. Yang, R. Lu, F. Gai, P. C. Xue, Y. Zhan, *Chem. Commun.* **2010**, *46*, 1088–1090; f) P. C. Xue, R. Lu, X. Yang, L. Zhao, D. Xu, Y. Liu, H. Zhang, H. Nomoto, M. Takafuji, H. Ihara, *Chem. Eur. J.* **2009**, *15*, 9824–9835.
- [8] a) Q. Tang, H. Li, Y. Liu, W. Hu, *J. Am. Chem. Soc.* **2006**, *128*, 14634–14639; b) A. L. Briseno, S. C. B. Mannsfeld, X. Lu, Y. Xiong, S. A. Jenekhe, Z. Bao, Y. Xia, *Nano Lett.* **2007**, *7*, 668–675; c) A. L. Briseno, C. Reese, J. M. Hancock, S. C. B. Mannsfeld, Y. Xiong, S. A. Jenekhe, Z. Bao, Y. Xia, *Nano Lett.* **2007**, *7*, 2847–2853; d) A. L. Briseno, S. C. B. Mannsfeld, S. A. Jenekhe, Z. Bao, Y. Xia, *Mater. Res. Materials Today* **2008**, *11*, 38–47; e) A. L. Briseno, S. C. B. Mannsfeld, P. J. Shamberger, F. S. Ohuchi, Z. Bao, S. A. Jenekhe, Y. Xia, *Chem. Mater.* **2008**, *20*, 4712–4719.
- [9] a) H. Xin, F. S. Kim, S. A. Jenekhe, *J. Am. Chem. Soc.* **2008**, *130*, 5424–5425; b) H. Xin, G. Ren, F. S. Kim, S. A. Jenekhe, *Chem. Mater.* **2008**, *20*, 6199–6207; c) S. Berson, R. D. Bettignies, S. Bailly, S. Guillerez, *Adv. Funct. Mater.* **2007**, *17*, 1377–1384.
- [10] a) H. Wang, Q. Liao, H. Fu, Y. Zeng, Z. Jiang, J. Ma, J. Yao, *J. Mater. Chem.* **2009**, *19*, 89–96; b) Y. Zhao, A. Peng, H. Fu, Y. Ma, J. Yao, *Adv. Mater.* **2008**, *20*, 1661–1665; c) Y. Zhao, J. Xu, A. Peng, H. Fu, Y. Ma, L. Jiang, J. Yao, *Angew. Chem.* **2008**, *120*, 7411–7415; *Angew. Chem. Int. Ed.* **2008**, *47*, 7301–7305; d) Q. Liao, H. Fu, J. Yao, *Adv. Mater.* **2009**, *21*, 4153–4157; e) Y. Che, X. Yang, K. Balakrishnan, J. Zuo, L. Zang, *Chem. Mater.* **2009**, *21*, 2930–2934; f) K. Takazawa, Y. Kitahama, Y. Kimura, G. Kido, *Nano Lett.* **2005**, *5*, 1293–1296.
- [11] a) Y. Che, A. Datar, K. Balakrishnan, L. Zang, *J. Am. Chem. Soc.* **2007**, *129*, 7234–7235; b) Y. Che, X. Yang, G. Liu, C. Yu, H. Ji, J. Zuo, L. Zang, *J. Am. Chem. Soc.* **2010**, *132*, 5743–5750; c) K. Balakrishnan, A. Datar, R. Oitker, H. Chen, J. Zuo, L. Zang, *J. Am. Chem. Soc.* **2005**, *127*, 10496–10497; d) A. Datar, R. Oitker, L. Zang, *Chem. Commun.* **2006**, 1649–1651.
- [12] Y. Zhao, H. Fu, F. Hu, A. Peng, J. Yao, *Adv. Mater.* **2007**, *19*, 3554–3558.
- [13] C. Vijayakumar, V. K. Praveen, A. Ajayaghosh, *Adv. Mater.* **2009**, *21*, 2059–2063.
- [14] a) J. Kido, Y. Okamoto, *Chem. Rev.* **2002**, *102*, 2357–2368; b) M. R. Robinson, M. B. O'Reagan, G. C. Bazan, *Chem. Commun.* **2000**, 1645–1646.
- [15] a) K. Ono, K. Yoshikawa, Y. Tsuji, H. Yamaguchi, R. Uozumi, M. Tomura, K. Taga, K. Saito, *Tetrahedron* **2007**, *63*, 9354–9358; b) E. Cogné-Laage, J. F. Allemand, O. Ruel, J.-B. Baudin, V. Croquette, M. Blanchard-Desce, L. Jullien, *Chem. Eur. J.* **2004**, *10*, 1445–1455; c) G. Zhang, J. Chen, S. J. Payne, S. E. Kooi, J. N. Demas, C. L. Fraser, *J. Am. Chem. Soc.* **2007**, *129*, 8942–8943; d) B. Domercq, C. Grasso, J.-L. Maldonado, M. Halik, S. Barlow, S. R. Marder, B. Kippelen, *J. Phys. Chem. B* **2004**, *108*, 8647–8651; e) M. Halik, W. Wenseleers, C. Grasso, F. Stellacci, E. Zojer, S. Barlow, J.-L. Brédas, J. W. Perry, S. R. Marder, *Chem. Commun.* **2003**, 1490–1491; f) H. Maeda, Y. Mihashi, Y. Haketa, *Org. Lett.* **2008**, *10*, 3179–3182.
- [16] a) A. Nagai, K. Kokado, Y. Nagata, M. Arita, Y. Chujo, *J. Org. Chem.* **2008**, *73*, 8605–8607; b) A. Nagai, K. Kokado, Y. Nagata, Y. Chujo, *Macromolecules* **2008**, *41*, 8295–8298.
- [17] J. Emsley, *Struct. Bonding (Berlin)* **1984**, *57*, 147–191.
- [18] G. Gilli, F. Bellucci, V. Ferretti, V. Bertolasi, *J. Am. Chem. Soc.* **1989**, *111*, 1023–1028.
- [19] L. Zhao, W. Yang, Y. Luo, T. Zhai, G. Zhang, J. Yao, *Chem. Eur. J.* **2005**, *11*, 3773–3778.
- [20] a) S. A. Jenekhe, L. Lu, M. M. Alam, *Macromolecules* **2001**, *34*, 7315–7324; b) B. Huang, J. Li, Z. Jiang, J. Qin, G. Yu, Y. Liu, *Macromolecules* **2005**, *38*, 6915–6922.
- [21] a) A. Langendoen, J. P. M. Plug, G. J. Koomen, U. K. Pandit, *Tetrahedron* **1989**, *45*, 1759–1762; b) T. Xu, R. Lu, X. Qiu, X. Liu, P. Xue, C. Tan, C. Bao, Y. Zhao, *Eur. J. Org. Chem.* **2006**, 4014–4020.
- [22] S. Li, G. Zhong, W. Zhu, F. Li, J. Pan, W. Huang, H. Tian, *J. Mater. Chem.* **2005**, *15*, 3221–3228.
- [23] M. Maiti, T. Misra, T. Bhattacharya, C. Basu (nee Deb), A. De, S. K. Sarkar, T. Ganguly, *J. Photochem. Photobiol.* **2002**, *152*, 41–52.
- [24] a) G. Jones II., W. R. Jackson, C. Choi, W. R. Bergmark, *J. Phys. Chem.* **1985**, *89*, 294–300; b) S. Nad, H. Pal, *J. Phys. Chem. A* **2001**, *105*, 1097–1106; c) F. Loiseau, S. Campagna, A. Hameurlaine, W. Dehaen, *J. Am. Chem. Soc.* **2005**, *127*, 11352–11363.
- [25] M. Maus, W. Rettig, D. Bonafoux, R. Lapouyade, *J. Phys. Chem. A* **1999**, *103*, 3388–3401.
- [26] J. S. Yang, K. L. Liao, C. M. Wang, C. Y. Hwang, *J. Am. Chem. Soc.* **2004**, *126*, 12325–12335.
- [27] C. Reichardt, *Chem. Rev.* **1994**, *94*, 2319–2358.
- [28] N. Mataga, T. Kubota, *Molecular Interactions and Electronic Spectra*, Dekker, New York, **1970**.
- [29] R. K. Chen, G. J. Zhao, X. C. Yang, X. Jiang, J. F. Liu, H. N. Tian, Y. Gao, X. Liu, K. Han, M. T. Sun, L. C. Sun, *J. Mol. Struct.* **2008**, *876*, 102–109.
- [30] a) Z. Tian, Y. Chen, W. Yang, J. Yao, L. Zhu, Z. Shuai, *Angew. Chem.* **2004**, *116*, 4152–4155; *Angew. Chem. Int. Ed.* **2004**, *43*, 4060–4063; b) J. Wang, Y. Zhao, J. Zhang, J. Zhang, B. Yang, Y. Wang, D. Zhang, H. You, D. Ma, *J. Phys. Chem. C* **2007**, *111*, 9177–9183.

- [31] a) M. George, R. G. Weiss, *Chem. Mater.* **2003**, *15*, 2879–2888; b) Y. Zhou, T. Yi, T. Li, Z. Zhou, F. Li, W. Huang, C. Huang, *Chem. Mater.* **2006**, *18*, 2974–2981.
- [32] a) E. Rousseau, M. Van der Auweraer, F. C. De Schryver, *Langmuir* **2000**, *16*, 8865–8870; b) T. E. Kaiser, V. Stepanenko, F. Würthner, *J. Am. Chem. Soc.* **2009**, *131*, 6719–6732.
- [33] a) X. Q. Li, V. Stepanenko, Z. Chen, P. Prins, L. D. A. Siebbeles, F. Würthner, *Chem. Commun.* **2006**, 3871–3873; b) S. Ghosh, X. Q. Li, V. Stepanenko, F. Würthner, *Chem. Eur. J.* **2008**, *14*, 11343–11357.
- [34] a) R. F. Fink, J. Seibt, V. Engel, M. Renz, M. Kaupp, S. Lochbrunner, H. M. Zhao, J. Pfister, F. Würthner, B. Engels, *J. Am. Chem. Soc.* **2008**, *130*, 12858–12859; b) Z. Chen, V. Stepanenko, V. Dehm, P. Prins, L. D. A. Siebbeles, J. Seibt, P. Marquetand, V. Engel, F. Würthner, *Chem. Eur. J.* **2007**, *13*, 436–449.
- [35] a) D. G. Whitten, *Acc. Chem. Res.* **1993**, *26*, 502–509; b) L. Lu, T. M. Cocker, R. E. Bachman, R. G. Weiss, *Langmuir* **2000**, *16*, 20–34.
- [36] F. Würthner, *Chem. Commun.* **2004**, 1564–1579.
- [37] a) I. Nakazawa, M. Masuda, Y. Okada, T. Hanada, K. Yase, M. Asai, T. Shimizu, *Langmuir* **1999**, *15*, 4757–4764; b) M. Masuda, V. Vill, T. Shimizu, *J. Am. Chem. Soc.* **2000**, *122*, 12327–12333.
- [38] M. Teng, K. G. ang, X. Jia, M. Gao, Y. Li, Y. Wei, *J. Mater. Chem.* **2009**, *19*, 5648–5654.
- [39] K. Brunner, A. van Dijken, H. Börner, J. J. A. M. Bastiaansen, N. M. M. Kiggen, B. M. W. Langeveld, *J. Am. Chem. Soc.* **2004**, *126*, 6035–6042.
- [40] S. D. Dreher, D. J. Weix, T. J. Katz, *J. Org. Chem.* **1999**, *64*, 3671–3678.
- [41] R. Gujadhur, D. Venkataraman, J. T. Kintigh, *Tetrahedron Lett.* **2001**, *42*, 4791–4793.

Received: July 1, 2010
Published online: January 5, 2011